Supplementary Information

Direct Conversion of Cellulose to High-Yield Methyl Lactate over Ga-doped Zn/H-Nanozeolite Y Catalysts in Supercritical Methanol

Deepak Verma,[a,b] Rizki Insyani,[a] Young-Woong Suh,[c] Seung Min Kim,[d] Seok Ki Kim,[e] Jaehoon Kim*,[a,b]

[a] SKKU Advanced Institute of Nanotechnology (SAINT), Sungkyunkwan University,
2066 Seobu-Ro, Jangan-Gu, Suwon, Gyeong Gi-Do, 16419, Republic of Korea
[b] School of Mechanical Engineering, Sungkyunkwan University,
2066 Seobu-Ro, Jangan-Gu, Suwon, Gyeong Gi-Do, 16419, Republic of Korea
[c] Department of Chemical Engineering, Hanyang University,
[d] Institute of Advanced Composite Materials, Korea Institute of Science and Technology,
Chudong-ro 92, Bongdong-eup, Wanju-gun, Jeonranbuk-do, Republic of Korea
222 Wangsimni-ro, Seongdong-gu, Seoul 04763, Republic of Korea
[e] Carbon Resource Institute, Korea Research Institute of Chemical Technology,
141 Gajeongro, Yuseong, Daejeon 34114, Republic of Korea

Table S1. Comparison of the yields and conversion for lactic acid or its derivatives with the use of homogeneous and heterogeneous catalysts from various biomass-derived feedstocks.

	Feed	**Catalyst**	**Solvent**	**T (°C)**	**P_{N2} (MPa)**	**Time (h)**	**Conversion (%)**	**Yield (%) (Product name)**	**Reference**
Homogeneous catalysts	Glucose	$PbCl_2$	H_2O	170	3	2	>96	70.0 (LA)	Wang et al., 2013[1]
	Cellulose(ball milling)	$PbCl_2$	H_2O	190	3	4	-	68.0 (LA)	Wang et al., 2013[1]
	Cellulose (microcrystalline)	$PbCl_2$	H_2O	190	3	15	-	62.0 (LA)	Wang et al., 2013[1]
	Cellulose	$Er(OTf)_3$	H_2O	240	2	0.5	100	89.6 (LA)	Wang et al., 2013[2]
	Glycerol	Ir-based polymer/KOH	None	160	-	15	34.8	95.0(LA)	Sharninghausenet al., 2014[3]
	Cellulose	Er-K10	H_2O	240	2	0.5	100	67.6 (LA)	Wang et al., 2015[4]
	Sugars (fructose and sucrose)	In–Sn-based catalyst/$NaBF_4$	MeOH	120-190	0.5	10	>95	72.0 (ML)	Nemoto et al., 2016[5]
Heterogeneous catalysts	Glucose	Zn–Sn–Beta zeolite	H_2O	190	-	2	>99	48.0 (LA)	Dong et al., 2016[6]
	Sucrose	Zn–Sn–Beta zeolite	H_2O	190	-	2	>99	54.0 (LA)	Dong et al., 2016[6]
	Cellulose	AlW	H_2O	190	5*	24	47	28.0 (LA)	Chambon et al., 2011[7]
	Cellulose	Nb@AlF_3	H_2O	180	-	24	>95	20.0 (LA)	Coman et al., 2015[8]
	Cellulose	Zr-SBA-15	95% EtOH	260	4	6	91.4	~33.0 (EL)	Yang et al., 2016[9]
	Cellulose	Zr-SBA-15	95% MeOH	240	4	10	100	28.1 (ML)	Yang et al., 2016[10]
	Cellulose	Ga-doped Zn/H-nanozeoliteY	MeOH	270	1	5	>99	57.8 (ML)	This study
	Glucose			270	1	1	100	64.0 (ML)	
	Fructose			270	1	1	100	67.3 (ML)	

LA, Lactic acid; ML, Methyl lactate; and EL, Ethyl lactate, *P_{He}

The conversion and yield of products from cellulose and lignocellulosic based biomass (oakwood) were calculated as follows;

Cellulose and oakwood biomass conversion (wt%)

$$X = 1 - \frac{Mass\ of\ unconverted\ reactatnt}{Mass\ of\ initial\ reactant} \times 100\%$$

Yield of products

Yield of ML, MMP, MLU and MDA from cellulose were calculated as follows:

$$ML\ yield\ (\%) = \frac{mole\ number\ of\ ML}{2 \times mol\ number\ of\ C_6H_{10}O_5\ unit} \times 100\%$$

$$MMP\ yield\ (\%) = \frac{mole\ number\ of\ MMP}{2\ \times mol\ number\ of\ C_6H_{10}O_5\ unit} \times 100\%$$

$$MLU\ yield\ (\%) = \frac{5\ x\ mole\ number\ of\ MLU}{6\ \times mol\ number\ of\ C_6H_{10}O_5\ unit} \times 100\%$$

$$MDA\ Yield\ (\%) = \frac{mole\ of\ MDA\ produced}{3 \times mole\ of\ C6\ unit}\ \times\ 100\%$$

In case of lignocellulosic-based raw biomass (oakwood), only holocellulose {containing cellulose (composed of C6 units) and hemicellulose (composed of C5 units)} can be converted into C2 (methyl dimethoxyacetate, MDA), C3 (Methyl lactate, ML; methyl 2-methoxypropionate, MMP) and C5 (methyl levulinate, MLU) products under the scMeOH condition, whereas other components such as lignin, and ash cannot be participated into these products. Therefore, the yield of these compounds were based on C6 and C5 monomeric units contained in the raw oakwood biomass using the following equation:

Yield of ML, MMA and MLU from oakwood biomass are based on C6 or C5 units;

$$ML\ Yield\ (\%) = \frac{mole\ of\ ML\ produced}{[2 \times (mole\ of\ C6\ unites)\ +\ (mole\ of\ C5\ unit)]}\ \times\ 100\%$$

$$MMA\ Yield\ (\%) = \frac{mole\ of\ MMA\ produced}{[2 \times (mole\ of\ C6\ unites)\ +\ (mole\ of\ C5\ unit)]} \times\ 100\%$$

$$MLU\ Yield\ (\%) = \frac{5\ x\ mole\ of\ MLU\ produced}{[6 \times (mole\ of\ C6\ unites)\ +\ (mole\ of\ C5\ unit)]} \times\ 100\%$$

The molecular weights of cellulose unit ($C_6H_{10}O_5$) and hemicellulose ($C_5H_8O_4$) were assumed to be 162 and 132 g mol^{-1}, respectively.

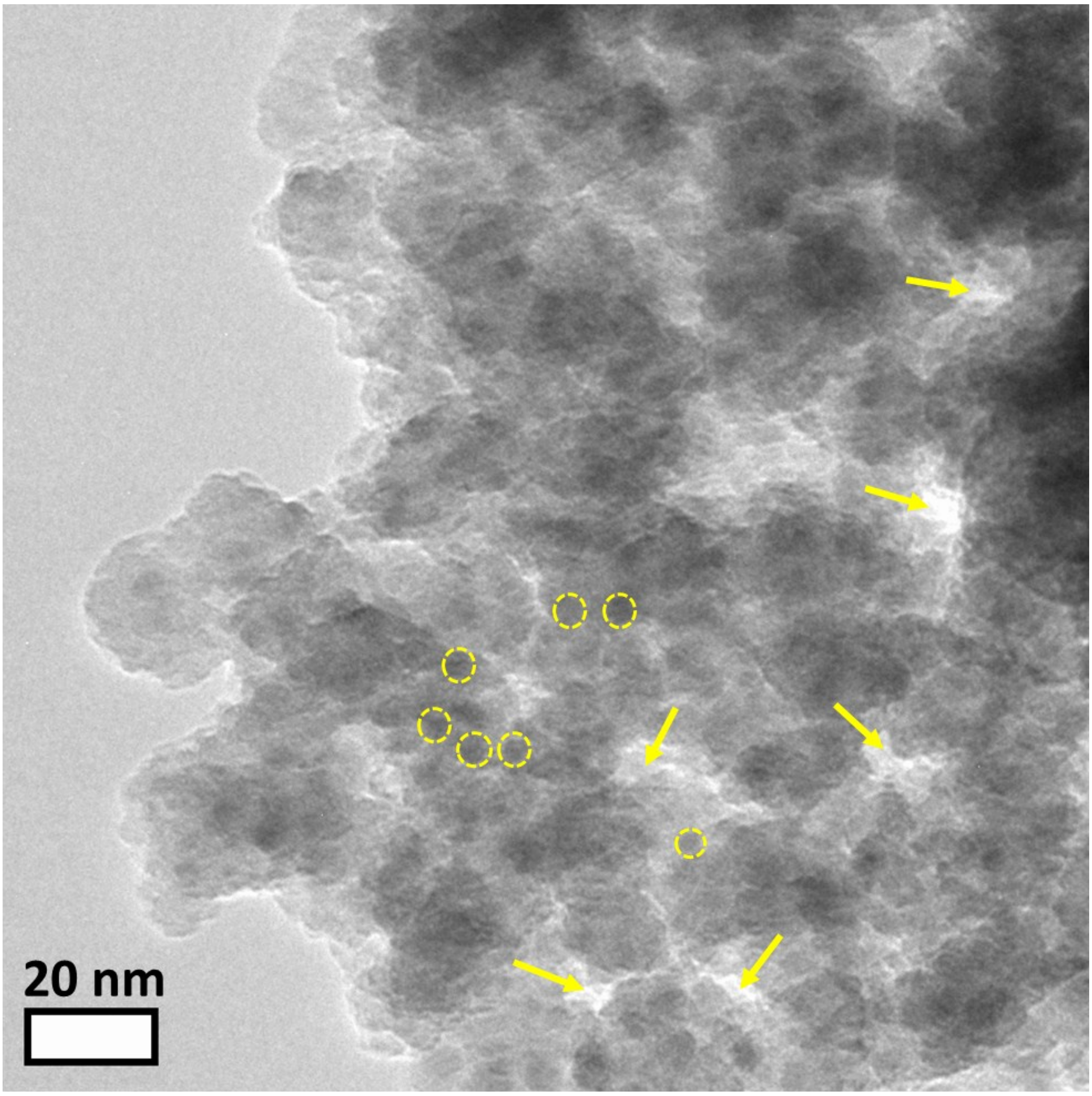

Fig. S1 High-magnification HRTEM image of the 20Z-2G catalyst. Yellow arrows and circles indicate the secondary mesopores and Zn/Ga oxide nanoparticles on the H-nanozeoliteY support, respectively.

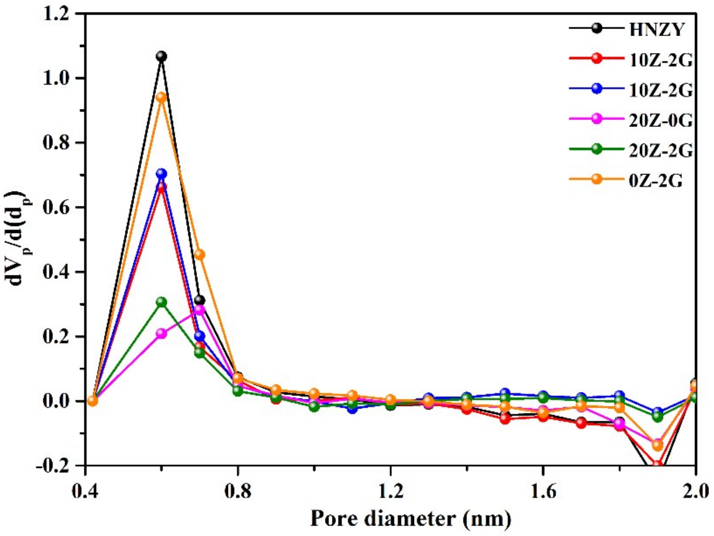

Fig. S2 Micropore size distribution determined using the MP model of the HNZY support and the Ga-doped Zn/HNZY catalysts.

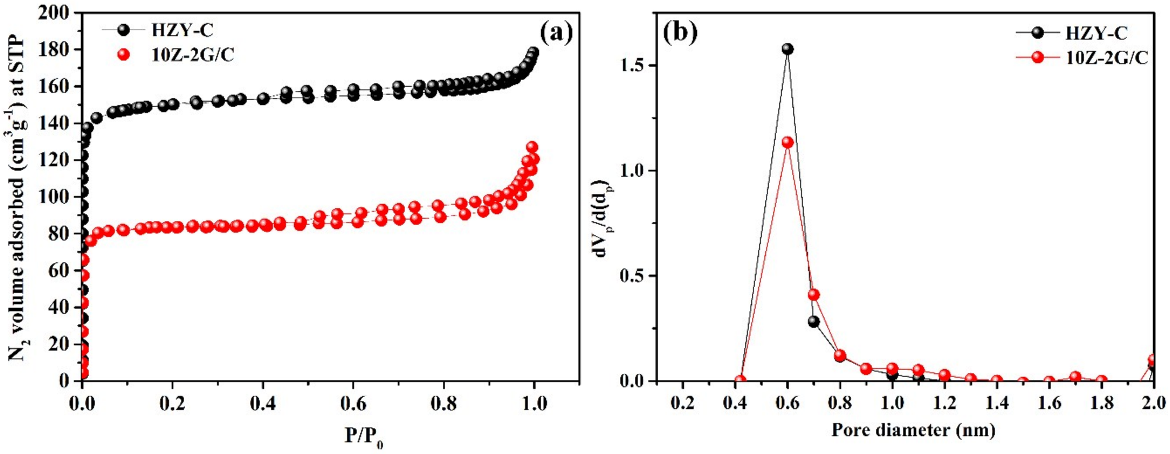

Fig. S3 (a) N_2 adsorption–desorption isotherms and (b) micropore size distributions determined using the MP model of HZY-C commercial support (CBV-600) and the 10Z-2G/C catalyst.

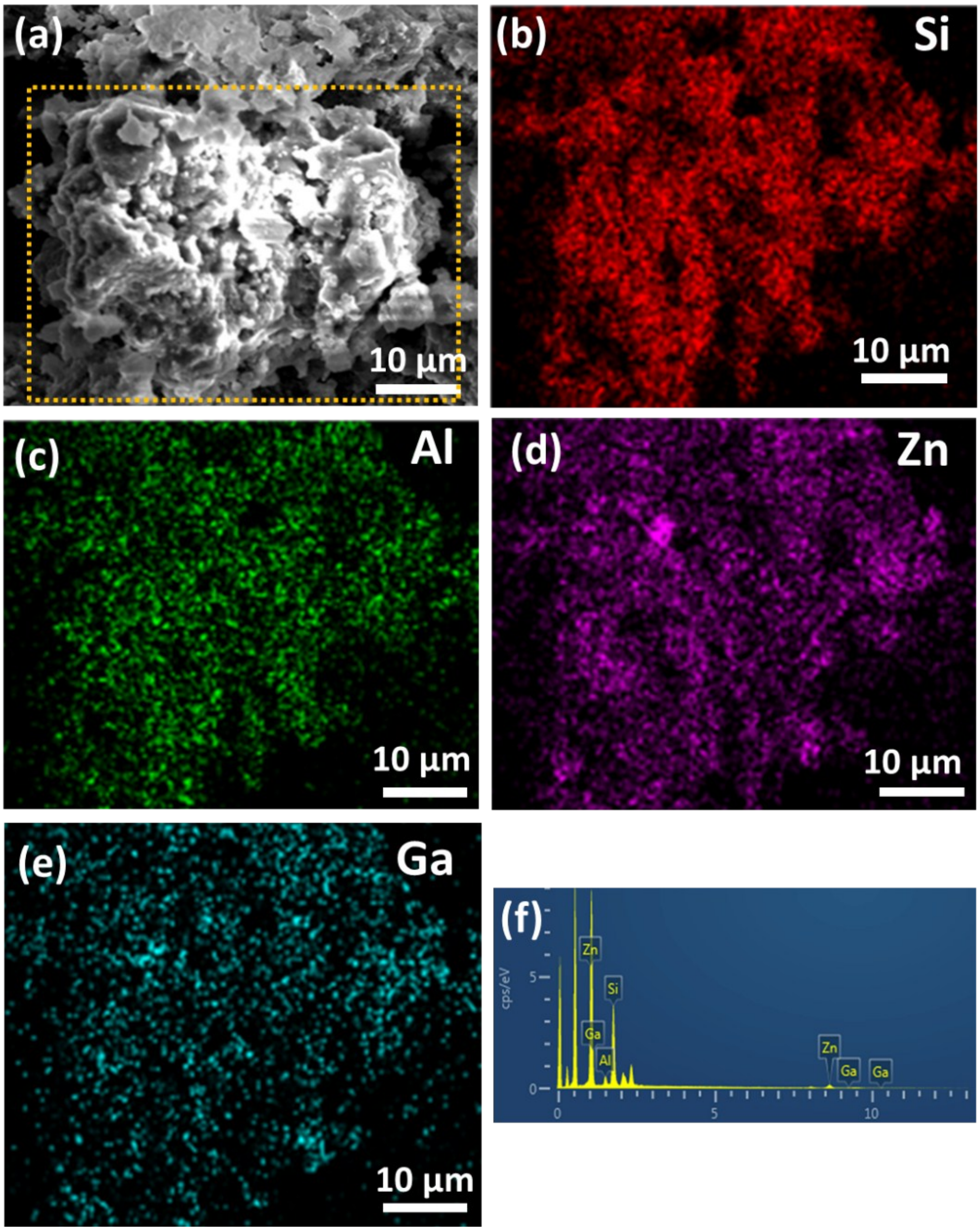

Fig. S4 (a) FE-SEM image, (b)–(e) elemental mapping of Si, Al, Zn, and Ga, respectively, and (f) corresponding EDS graph of the 10Z-2G catalyst.

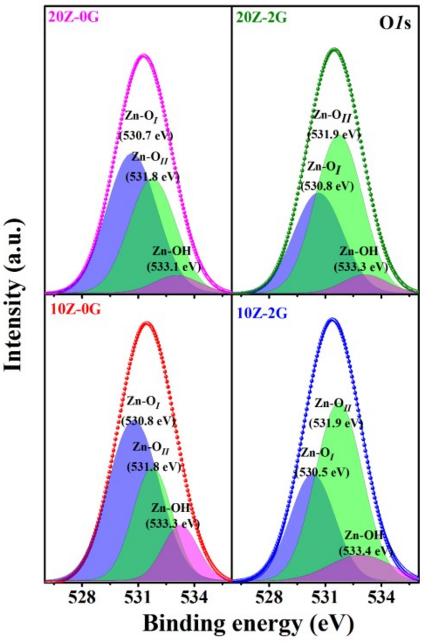

Fig. S5 O1s core-level peaks of the catalysts.

Table S2. Relative intensity of the O1s peaks of the catalysts evaluated by XPS.

	Fraction “O” state		
Catalyst	**Zn-O$_I$ (%)**	**Zn-O$_{II}$ (%)**	**Zn-OH (%)**
10Z-0G	50	38	12
10Z-2G	37	57	10
20Z-0G	49	42	9
20Z-2G	38	56	9

XPS analysis was employed to identify the change of distribution and content of surface oxygen species in the Ga-doped Zn/HNZY catalysts. The O 1s peaks were attributed to the HNZY support (such as SiO_2[11]and Al_2O_3). Under the assumption of the identical contribution of the HNZY support to each of the O 1s peak, the effect of Ga doping on ZnO was analyzed. As shown in Fig. S3, the typical O 1s peaks exhibited an asymmetric shape and was fitted well by three Gaussian peaks, centered at 530.7 eV (Zn-O$_I$), 531.8 eV (Zn-O$_{II}$), and 533.1 eV (Zn-OH), respectively.[12-13] These peaks were attributed to the oxidized metal ions in the ZnO lattice. Among these three well-identified Gaussian peaks, the low (Zn-O$_I$) and medium (Zn-O$_{II}$) binding-energy (BE) components were attributed to bulk $O^{2-}$and O^{2-} in the oxygen-deficient region in the ZnO lattice, respectively, while the highest (Zn-OH) BE was attributed to the chemisorbed or dissociated oxygen or –OH bonds on the ZnO surface.[14] The intensities of these three O 1s Gaussian peaks of ZnO were affected by Ga doping, as shown in Fig. S3. As compared with those of the 10Z-0G and 20Z-0G catalysts, the O1s peaks of the 10Z-2G and 20Z-2G catalysts were slightly shifted toward higher BEs, attributed to the difference in the electronegativity between Zn and Ga.[15] Moreover, the relative intensity of medium Be component was also affected by gallium loading. As described in Table S2, the Ga-doped Zn/HNZY catalysts(10Z-2G and 20Z-2G) exhibited a higher value of the Zn-O$_{II}$ component as compared with those of the Zn/HNZY catalyst without Ga doping (10Z-0G and 20Z-0G), indicating that Ga loading can create new oxygen vacancies after incorporation into the ZnO crystal lattice.[16] The high concentration of oxygen vacancies provides more active sites for the adsorption of reactants, which is important for the selective conversion of biomass.

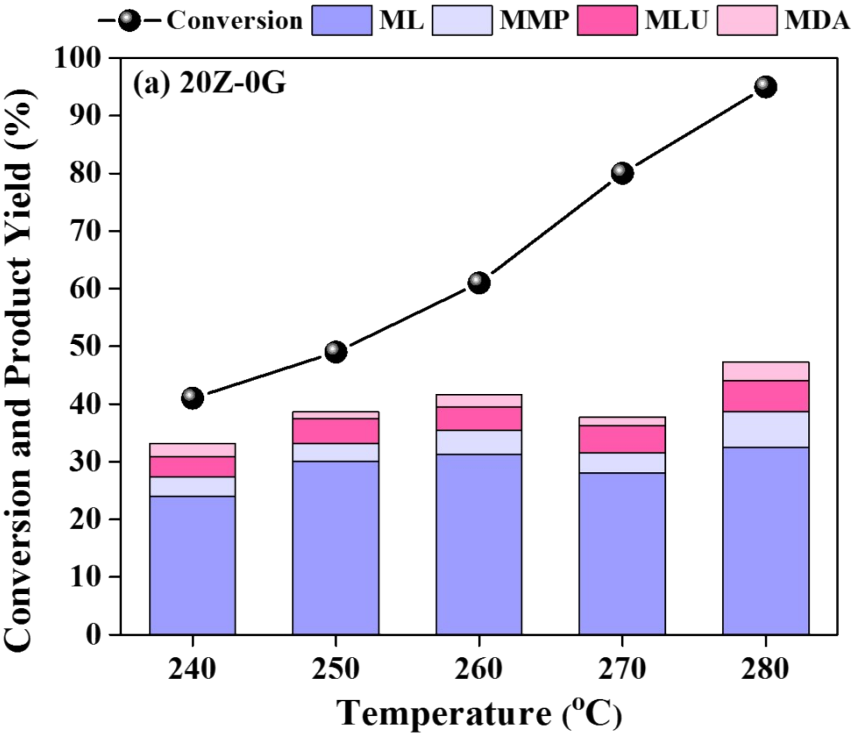

Fig. S6 Conversion of cellulose and yields of products over the 20Z-0G catalyst at varying reaction temperatures at a fixed reaction time of 5 h. Reaction conditions; 2 g of cellulose, 75 mL of MeOH, 0.5 g of catalyst, and an initial N_2 pressure of 1 MPa. ML, methyl lactate; MMP, methyl-2-methoxypropionate, MLU, methyl levulinate; and MDA, methyl dimethoxyacetate.

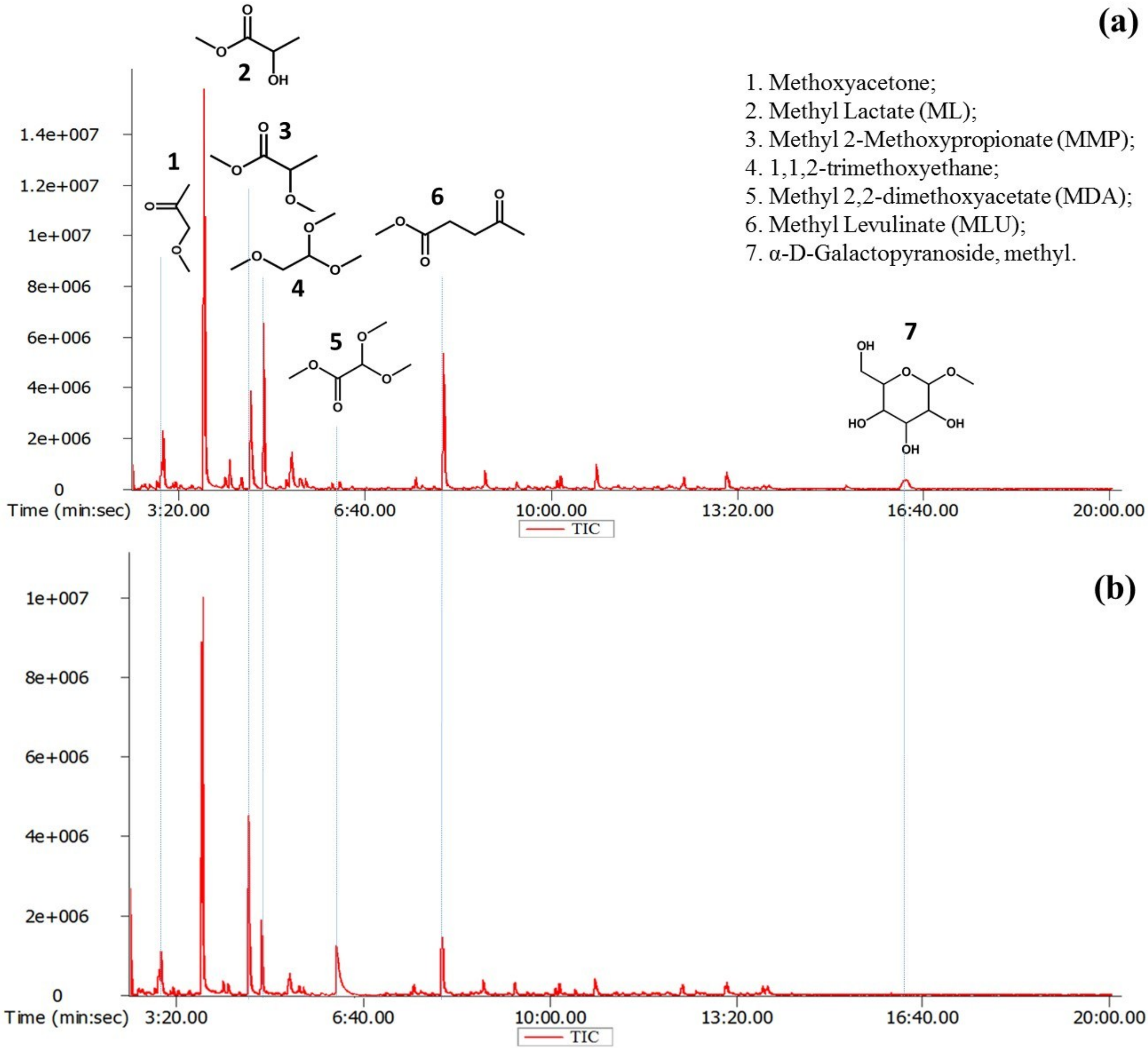

Fig. S7 GC-TOF–MS chromatograms for the liquid products obtained from the conversion of cellulose over the 20Z-2G catalyst in scMeOH at (a) 240 °C and (b) 270 °C. Reaction conditions; 2.0 g of cellulose, 0.5 g of catalyst, 75 mL of MeOH, a N_2 pressure of 1 MPa, and a reaction time of 5 h.

Table S3 Chemical compounds in the liquid products based on GC-TOF–MS chromatogram over the 20Z-2G catalyst.

	Sample	240°C	280°C
Name of compound	**Retention time (min)**	**Area%**	**Area%**
Ethers			
2-Methoxyethanol	02:30.4	0.214	0.102
2,2-Dimethoxypropane	02:40.0	0.150	0.275
1,1-Dimethoxypropane	03:01.7	0.525	0.253
Methoxyacetone	03:03.5	3.872	2.031
3-methoxypentane	03:16.1	0.142	0.235
1,1,2-Trimethoxyethane	04:51.2	3.719	0.633
1,1-Dimethoxy-2-butene	09:23.2	0.711	0.855
Methyl 2,2-dimethyoxyacetate	06:10.1	0.089	6.871
Esters			
Methyl lactate	03:47.6	38.02	59.84
Methyl methoxyacetate	04:10.2	0.835	0.565
Methyl 2-methoxypropionate	04:37.5	7.102	12.32
Methyl 3-furoate	05:15.6	0.214	0.494
Methyl levulinate	08:04.8	19.32	7.812
Acids			
2-hydroxy-2-methylpropanoic acid	04:08.1	0.104	0.435
Methyl 2-hydroxy-3-methylbutanoate	06:27.4	0.101	n.d.
Furans			
1-(2-furanyl)ethanone	10:37.3	0.114	0.269
Dihydro-5-methyl-5-(2-methylpropyl)-2(3H)-furanone	12:20.6	0.127	0.262
á-methoxy-(S)-2-furanethanol	07:35.0	0.161	0.214
5-Methyl-2-furancarboxaldehyde	07:41.9	0.123	0.203
Furfural	05:21.4	0.319	0.121
Alcohols			
R-(−)-1,2-propanediol	04:14.8	0.600	0.012
Glycolaldehyde dimethyl acetal	04:42.4	0.137	0.103
Monosaccharides			
Methyl α-D-Galactopyranoside	16:22.0	1.508	n.d.

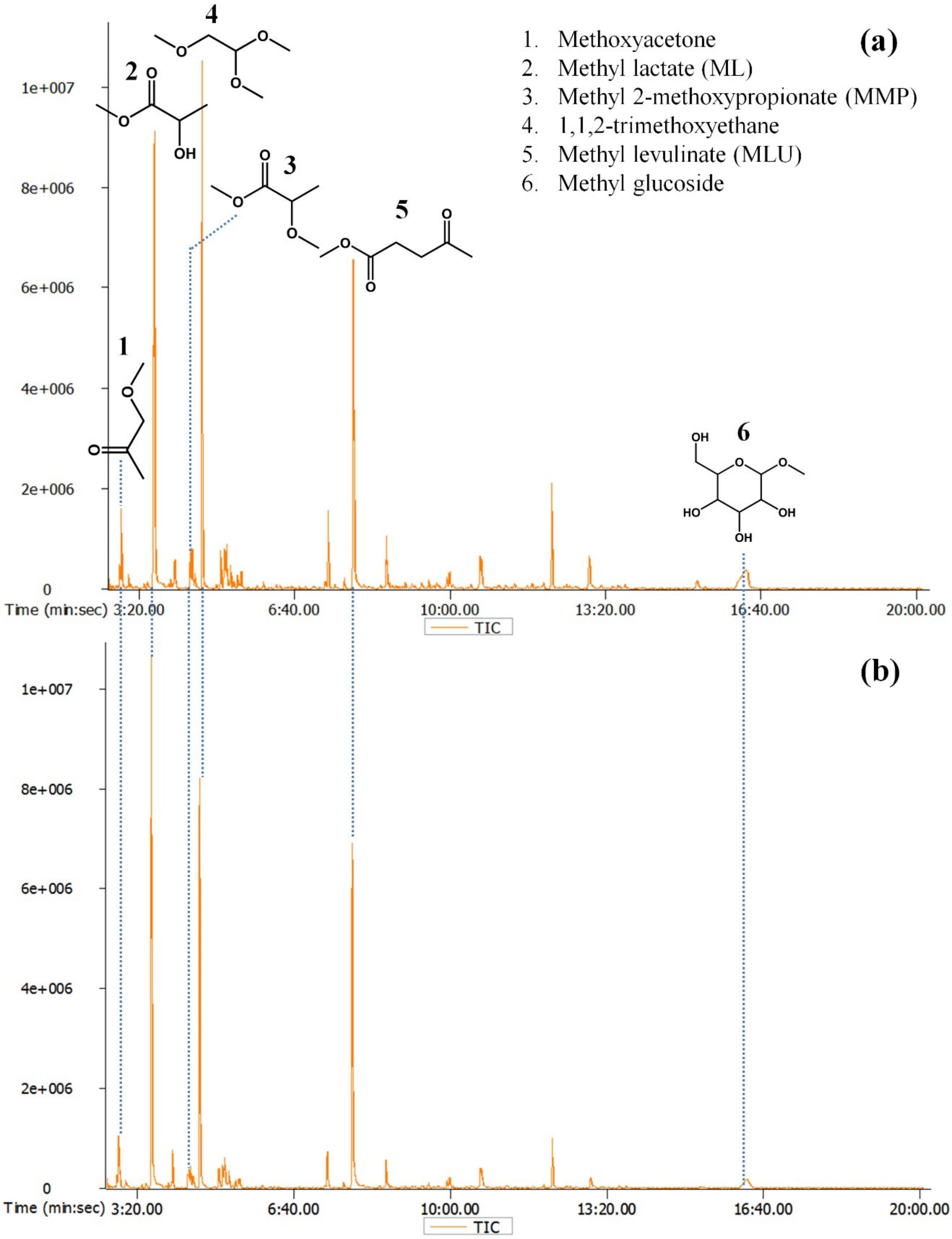

Fig. S8 GC-TOF–MS chromatograms for the liquid products obtained from the conversion of cellulose over the 10Z-2G/C catalyst in scMeOH at (a) 260 °C and (b) 270 °C. Reaction conditions; 2.0 g of cellulose, 0.5 g of catalyst, 75 mL of MeOH, a N_2 pressure of 1 MPa, and a reaction time of 5 h.

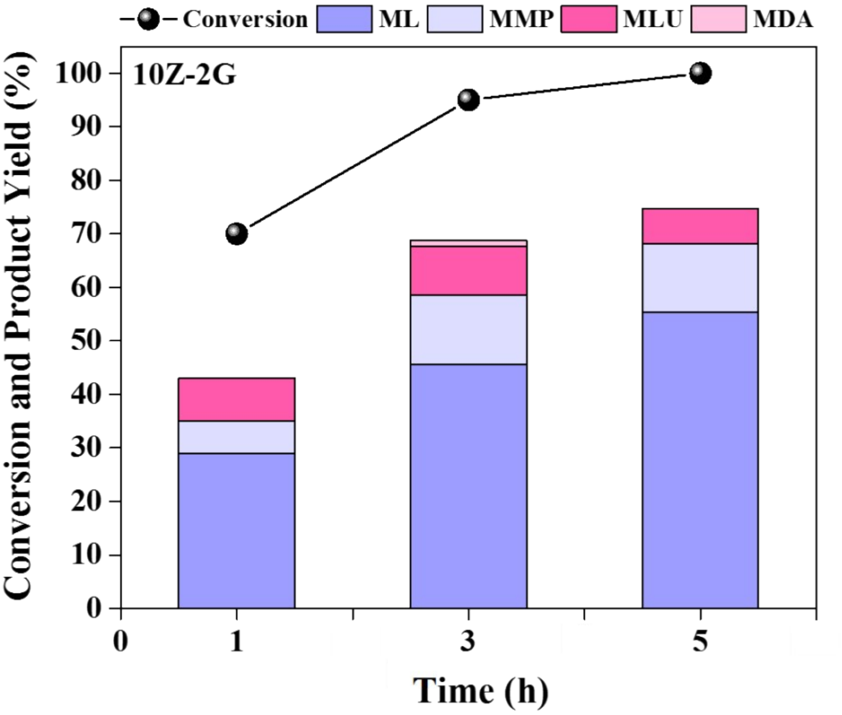

Fig. S9 Conversion of cellulose and yields of products over the 10Z-0G catalyst under varying reaction times at a fixed reaction temperature of 280 °C. Reaction conditions; 2 g of cellulose, 75 mL of MeOH, 0.5 g of catalyst, and an initial N_2 pressure of 1 MPa. ML, methyl lactate; MMP, methyl 2-methoxypropionate; MLU, methyl levulinate; and MDA, methyl dimethoxyacetate.

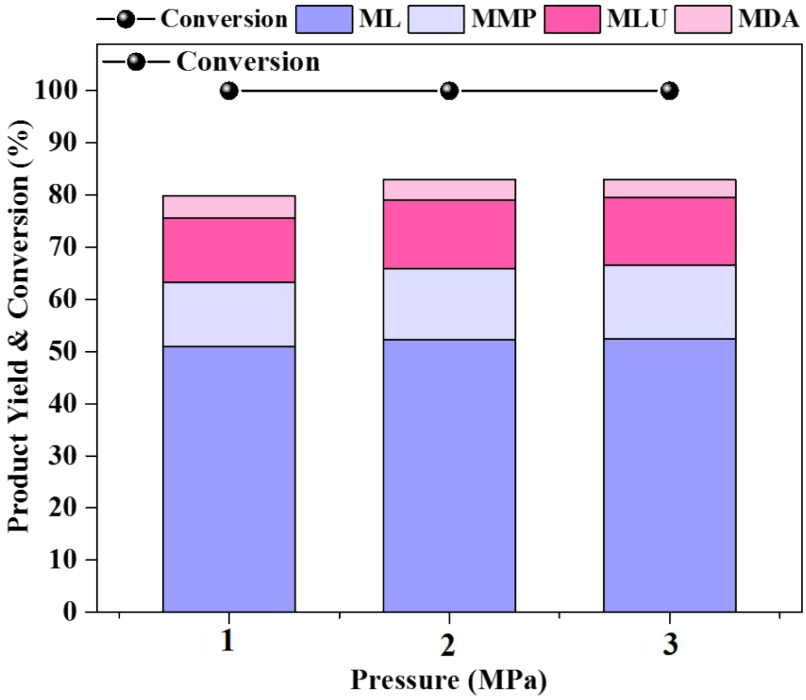

Fig. S10 Conversion and product yields obtained from the conversion of cellulose over the 20Z-2G catalyst under different initial reaction pressures at a fixed reaction temperature of 280 °C. Reaction conditions: 2 g of cellulose, 75 mL of MeOH, 0.5 g of catalyst, and a reaction time of 5 h. ML, methyl lactate; MMP, methyl 2-methoxypropionate; MLU, methyl levulinate; and MDA, methyl dimethoxyacetate.

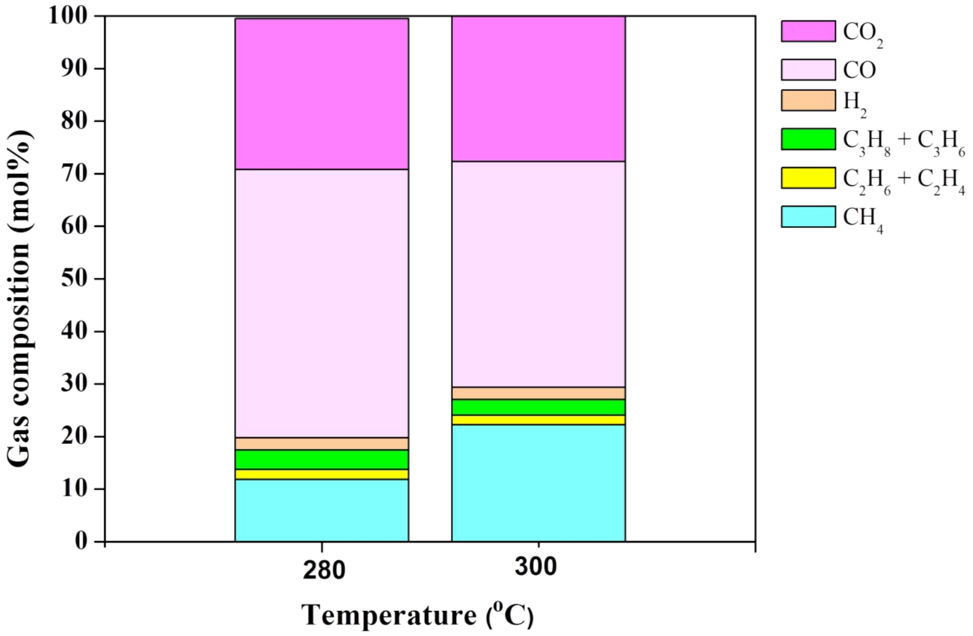

Fig. S11 Gaseous products obtained from the conversion of oakwood over the 10Z-2G catalyst under different reaction temperatures. Reaction conditions: 2.0 g of oakwood, 0.5 g of catalyst, 75mL of MeOH, N_2pressure of 1 MPa, and a reaction time of 1 h.

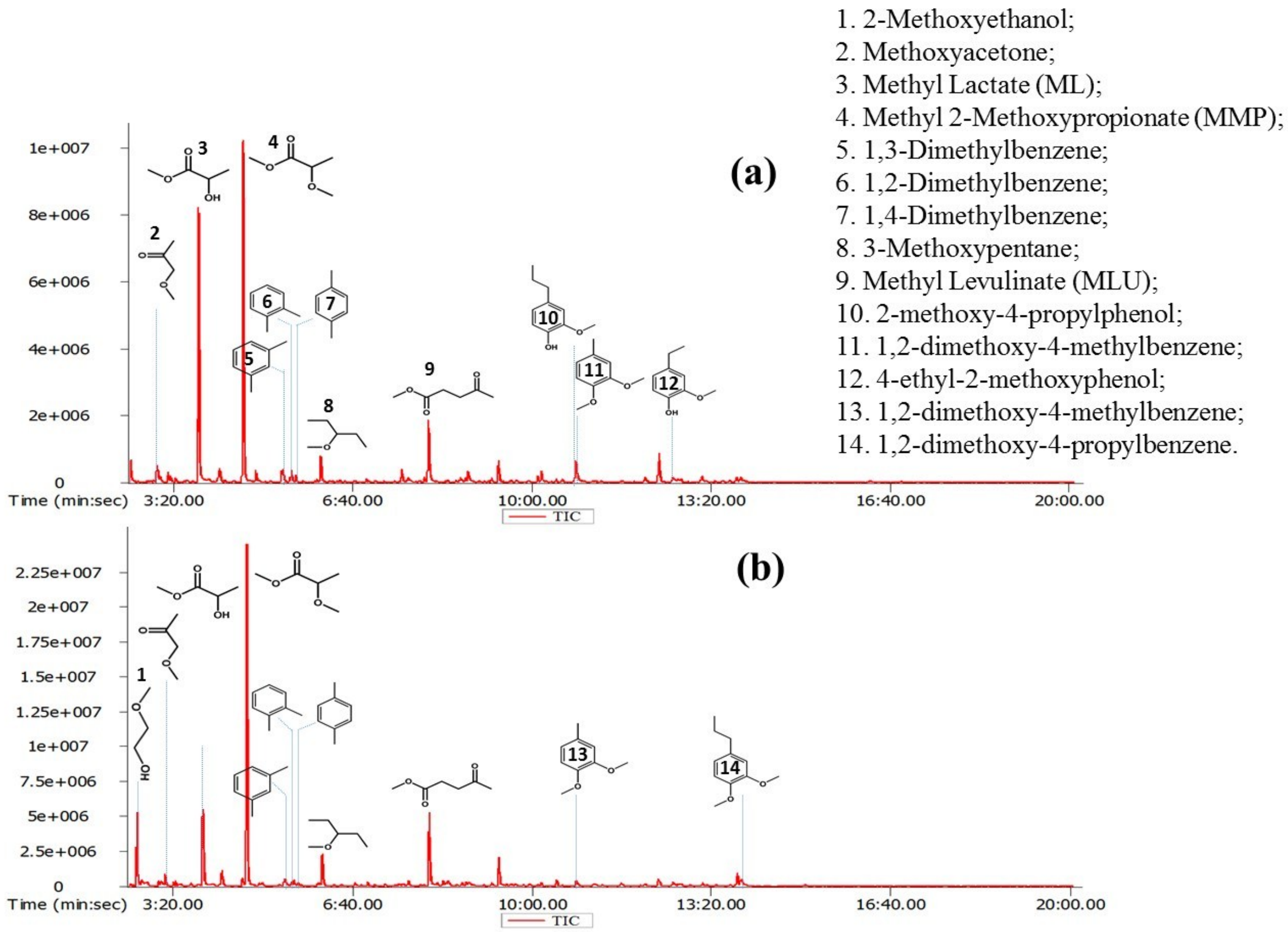

1. 2-Methoxyethanol;
2. Methoxyacetone;
3. Methyl Lactate (ML);
4. Methyl 2-Methoxypropionate (MMP);
5. 1,3-Dimethylbenzene;
6. 1,2-Dimethylbenzene;
7. 1,4-Dimethylbenzene;
8. 3-Methoxypentane;
9. Methyl Levulinate (MLU);
10. 2-methoxy-4-propylphenol;
11. 1,2-dimethoxy-4-methylbenzene;
12. 4-ethyl-2-methoxyphenol;
13. 1,2-dimethoxy-4-methylbenzene;
14. 1,2-dimethoxy-4-propylbenzene.

Fig. S12 GC-TOF–MS chromatogram of liquid products obtained from the conversion of raw oakwood sawdust using the 10Z-2G catalyst in scMeOH at different temperatures of (a) 280 °C and (b) 300 °C. Reaction conditions: 2.0 g of oakwood, 0.5 g of catalyst, 75 mL MeOH, an initial N_2 pressure of 1 MPa, and a reaction time of 1 h.

Table S4 Chemical compounds in the liquid products (area%) based on the GC-TOF–MS chromatograms from different feedstocks over the 10Z-2G catalyst.

	Sample	**Cellulose, 280 °C, 5h**	**Oakwood 300 °C, 1h**
Name of compound	**Retention time (min)**		
Ethers			
2-Methoxyethanol	02:30.4	0.214	5.182
2,2-Dimethoxypropane	02:40.0	0.150	1.255
1,2-Dimethoxyethane	02:43.6	0.208	0.564
1,1-Dimethoxy-2-methylpropane	04:27.5	0.109	0.234
1,2-Dimethoxyethene	02:59.1	0.115	0.625
1,1-Dimethoxypropane	03:01.7	0.525	1.056
Methoxyacetone	03:03.5	2.342	0.723
Methyl hydroxyacetate	03:13.2	0.165	0.865
2-Methoxy-1-propanol	03:16.1	0.142	0.235
1,1,2-Trimethoxyethane	04:51.2	3.719	0.633
3-Methoxypentane	06:04.8	0.211	2.532
3-Methoxyhex-1-ene	06:13.2	0.205	0.213
2-(2-methoxyethoxy)ethanol	08:49.1	0.317	0.311
1,2,4-Trimethoxybutane	09:23.2	0.211	2.855
Esters/Ketone			
Methyl 2-hydroxy-2-methylpropanoate	03:34.3	0.278	0.523
Methyl (2Z)-2-butenoate	03:41.7	0.097	0.025
Methyl lactate	03:47.6	68.02	11.24
Methyl methoxyacetate	04:10.2	0.135	0.565
Methyl 2-methoxypropionate	04:37.5	9.116	46.55
Methyl (+)-2-hydroxy-3-butenoate	05:15.6	0.214	0.594
Methyl 2-hydroxybutanoate	05:20.0	1.182	0.610
Methyl (3Z)-3-pentenoate	05:31.9	0.317	0.317
1,3-Dimethylbenzene	05:20.1	n.d.	0.403
1,2-Dimethylbenzene	05:32.3	n.d.	0.562
1,4-Dimethylbenzene	05:38.6	n.d.	0.620
Methyl 2-hydroxypentanoate	07:04.7	0.106	0.101
Methyl levulinate	08:04.8	7.241	11.56
Methyl 2-hydroxy-4-methylpentanoate	10:06.8	0.228	0.012
Dimethyl (3E)-3-hexenedioate	12:21.3	0.115	0.010
2-Cyclopenten-1-one	05:21.6	0.201	0.033
2-Butanone, 3-methoxy-3-methyl-	05:29.5	0.126	0.023
Acids			
Hydroxy-2-methylpropanoic acid	04:08.1	0.104	0.835
Furans			
1-(2-furanyl)-ethanone	10:37.3	0.114	0.369

2(3H)-Furanone, dihydro-5-methyl-5-(2-methylpropyl)-	12:20.6	0.127	0.562
2-Furanethanol, á-methoxy-(S)-	07:35.0	0.161	0.214
2-Furancarboxaldehyde, 5-methyl-	07:41.9	0.123	0.203
Methyl 2-furoate	07:54.3	0.201	0.300
Furfural	05:21.4	0.319	0.021
Alcohols			
R-(−)-1,2-Propanediol	04:14.8	0.600	0.012
Tetramethyl silicate	04:27.4	0.228	0.124
Glycolaldehyde dimethyl acetal	04:42.4	0.137	0.103
Monosaccharides			
D-Allose	15:17.3	n.d.	n.d.
α-D-Galactopyranoside, methyl	16:22.0	n.d.	n.d.
Aromatics			
1,2,3-Trimethoxy-5-methylbenzene	15.51.0	n.d.	0.010
Phenols	08.07.3	n.d.	0.210
4-Ethyl-2-methoxyphenol	13.50.2	n.d.	0.101
2-Methoxyphenol	09.47.0	n.d.	0.342
4-(1-Propen-1-yl)-1,2-benzenediol	15.12.3	n.d.	0.012
1,2-Dimethoxy-4-methylbenzene	10.86.2	n.d.	0.334
1,2-Dimethoxy-4-propylbenzene	14.05.3	n.d.	0.598

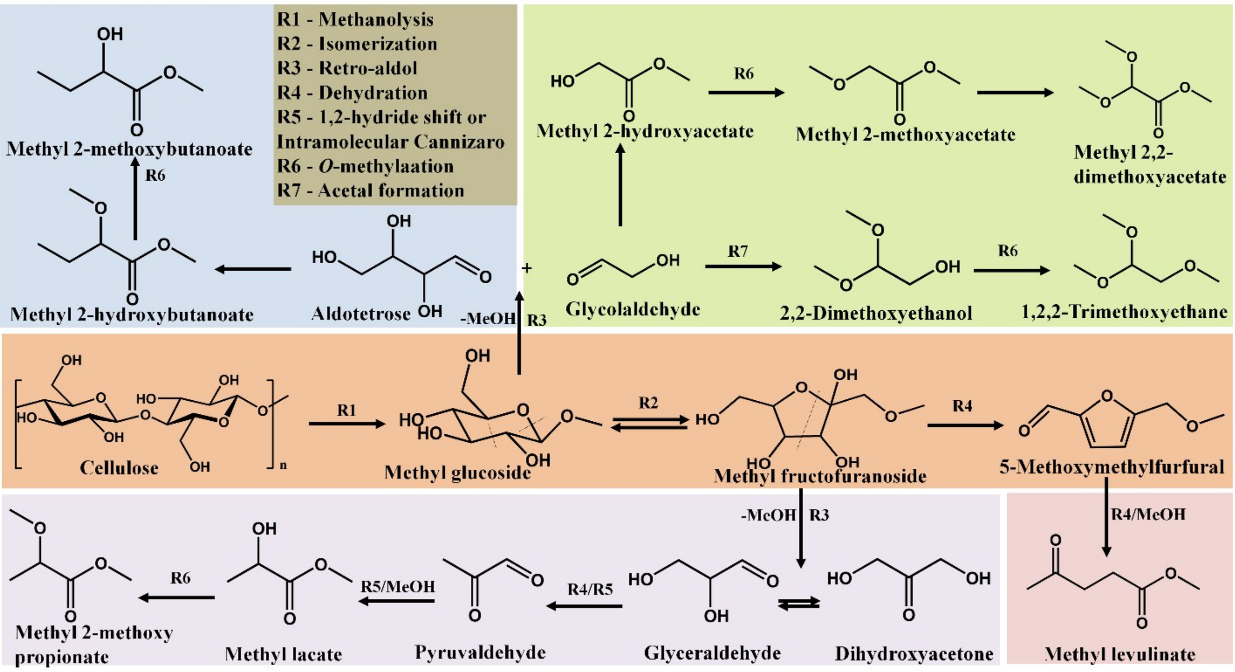

Scheme S1 Proposed reaction mechanisms for the acid-catalyzed production of methyl lactate from cellulose over Ga-doped Zn/HNZY in scMeOH. The chemicals encircled with dotted lines represent the major products, while those encircled with blue circles represent the minor products, as identified by GC-TOF–MS analysis (as shown in Fig. S5).

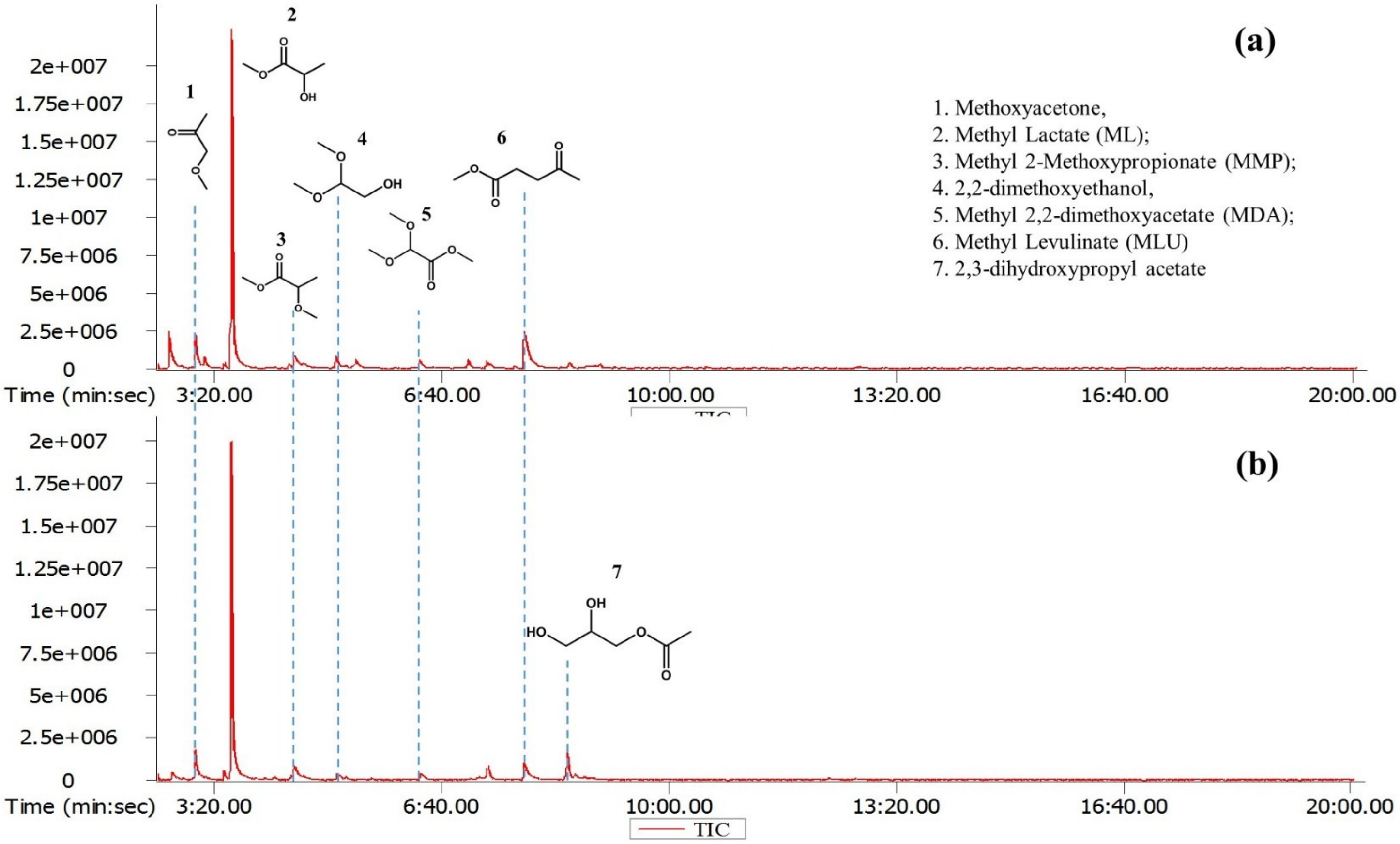

Fig. S13 GC-TOF–MS chromatograms of the liquid products obtained from the conversion of (a) glucose and (b) fructose over the 10Z-2G catalyst in scMeOH at 240 °C. Reaction conditions; 1.0 g of feedstock, 0.25 g of catalyst, 37.5 mL of MeOH, an initial N_2 pressure of 1 MPa, and a reaction time of 1 h.

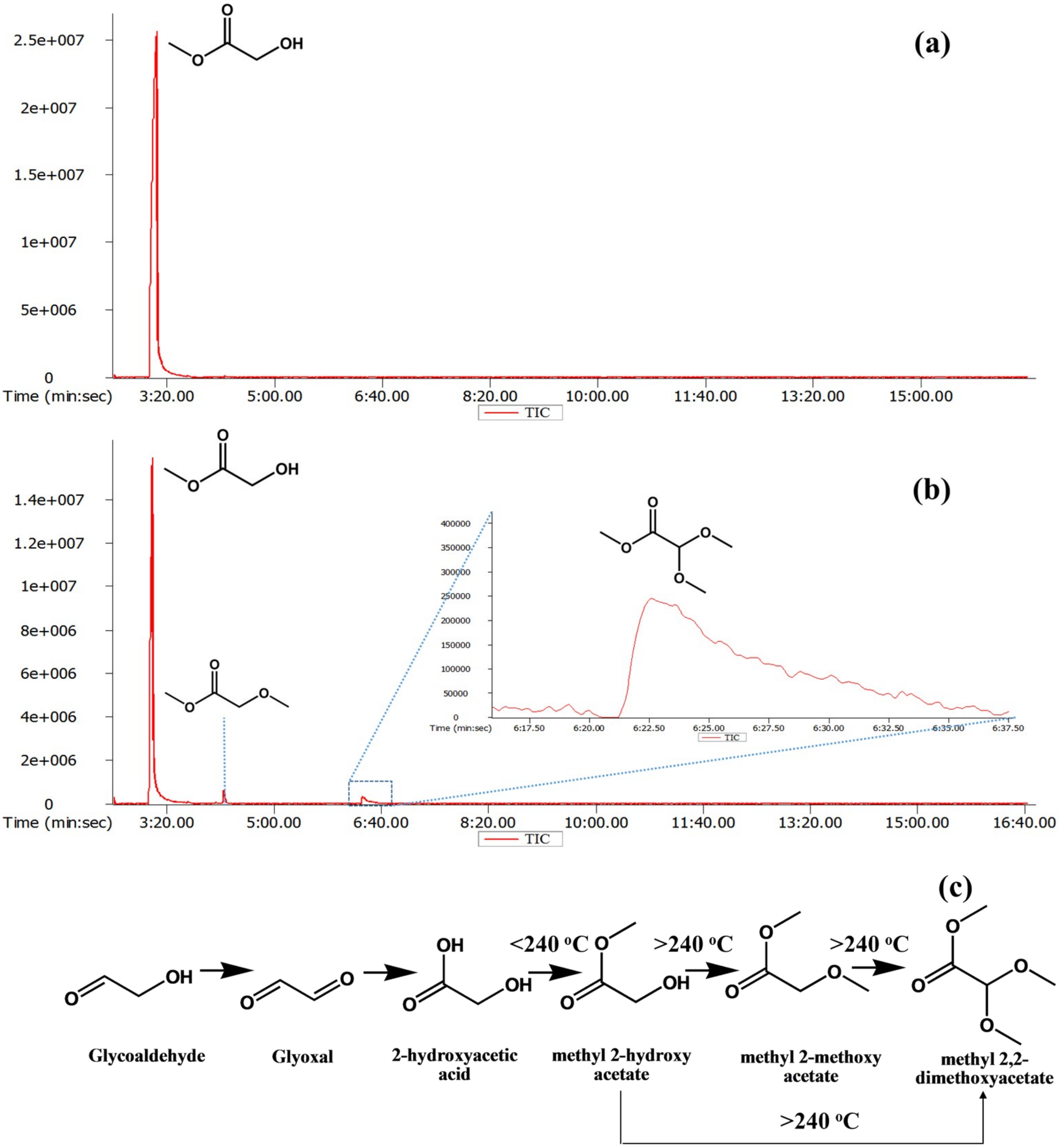

Fig. S14 GC-TOF–MS chromatograms of the liquid products obtained from the conversion of glyoxal (40% w/w) over the 10Z-2G catalyst in methanol at (a) 210 °C and (b) 240 °C. (c) Plausible reaction pathway from glycoladehyde to MDA. Reaction conditions; 1.0 g of glyoxal, 0.25 g of catalyst, 37.5 mL of MeOH, an initial N_2 pressure of 1 MPa, and a reaction time of 30 min.

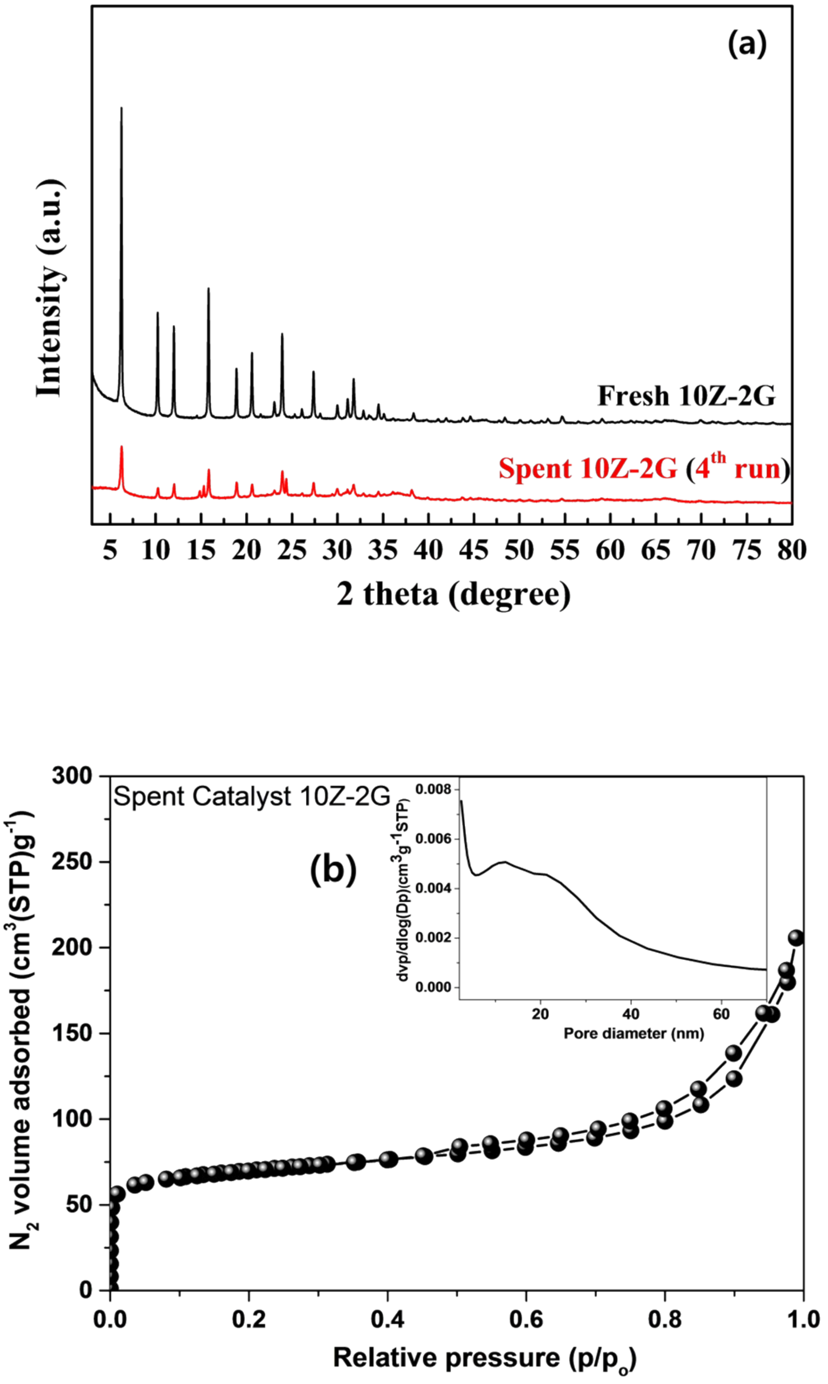

Fig. S15 (a) XRD patterns of the fresh and spent catalysts, (b) N_2 adsorption–desorption isotherm of the spent catalyst. The BJH plot is shown in the inset. After each reaction, the spent catalyst was regenerated by calcination in air at 550 °C for 4 h.

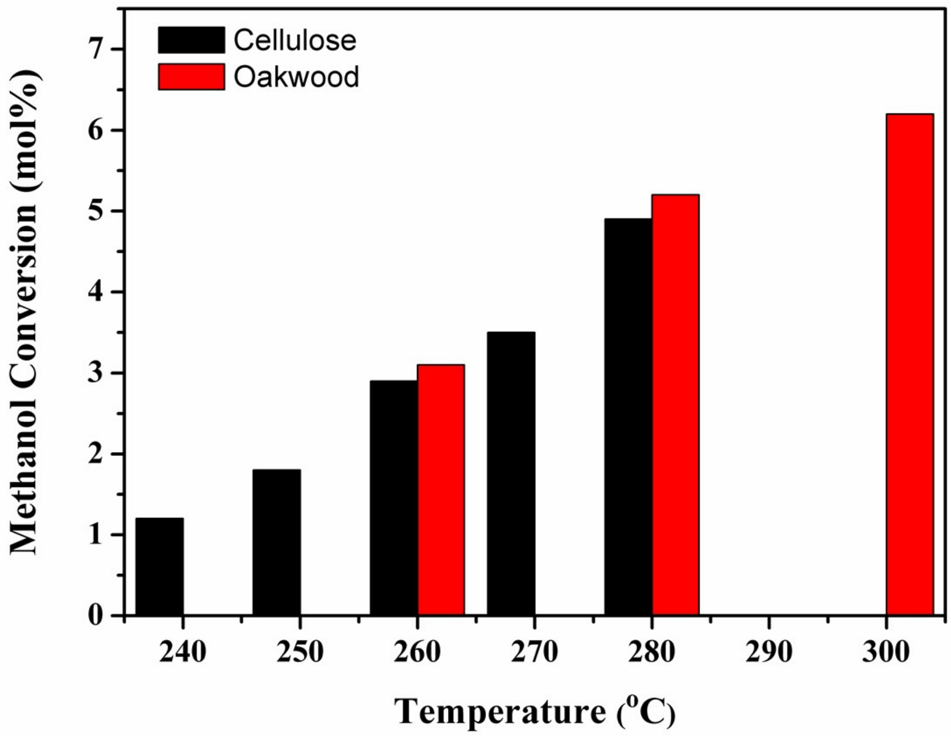

Fig. S16 The conversion of methanol (wt%) during the cellulose and oakwood reaction over the 10Z-2G catalyst. Reaction conditions; 2.0 g of feedstock, 0.5 g of catalyst, 75 mL of MeOH, an initial N_2 pressure of 1 MPa, and a reaction time of 5 h (for cellulose) or 1 h (for oakwood).

$$Methanol\ Conversion\ (\%) = \frac{X_0 - X_i}{X_0} \times 100\%$$

where,

X_0 = Total mole of the methanol before reaction

X_i = Total mole of the methanol after reaction

References

1. Wang, Y.; Deng, W.; Wang, B.; Zhang, Q.; Wan, X.; Tang, Z.; Wang, Y.; Zhu, C.; Cao, Z.; Wang, G., *Nat. Commun.* **2013,** *4*. 2141
2. Wang, F.-F.; Liu, C.-L.; Dong, W.-S., *Green Chem.* **2013,** *15*, 2091-2095.
3. Sharninghausen, L. S.; Campos, J.; Manas, M. G.; Crabtree, R. H., *Nat. Commun.* **2014,** *5*, 5084
4. Wang, F.-F.; Liu, J.; Li, H.; Liu, C.-L.; Yang, R.-Z.; Dong, W.-S., *Green Chem.* **2015,** *17*, 2455-2463.
5. Nemoto, K.; Hirano, Y.; Hirata, K.-i.; Takahashi, T.; Tsuneki, H.; Tominaga, K.-i.; Sato, K., *App. Catal. B* **2016,** *183*, 8-17.
6. Dong, W.; Shen, Z.; Peng, B.; Gu, M.; Zhou, X.; Xiang, B.; Zhang, Y., *Sci. Rep.* **2016,** *6*.
7. Chambon, F.; Rataboul, F.; Pinel, C.; Cabiac, A.; Guillon, E.; Essayem, N., *App. Cata. B* **2011,** *105*, 171-181.
8. Coman, S. M.; Verziu, M.; Tirsoaga, A.; Jurca, B.; Teodorescu, C.; Kuncser, V.; Parvulescu, V. I.; Scholz, G.; Kemnitz, E., *ACS Catal.* **2015,** *5*, 3013-3026.
9. Yang, L.; Yang, X.; Tian, E.; Lin, H., *ChemSusChem* **2016,** *9*, 36-41.
10. Yang, L.; Yang, X.; Tian, E.; Vattipalli, V.; Fan, W.; Lin, H., *J Catal* .**2016,** *333*, 207-216.
11. Barreca, D.; Gasparotto, A.; Maccato, C.; Tondello, E.; Rossetto, G., *Thin Solid Films* **2008,** *516*, 7393-7399.
12. De la Rosa, E.; Sepulveda-Guzman, S.; Reeja-Jayan, B.; Torres, A.; Salas, P.; Elizondo, N.; Yacaman, M. J., *J Phys. Chem. C* **2007,** *111*, 8489-8495.
13. Park, G. C.; Hwang, S. M.; Lim, J. H.; Joo, J., *Nanoscale* **2014,** *6*, 1840-1847.
14. Duan, X.; Song, C.; Yu, F.; Yuan, D.; Li, X., *App. Surf. Sci.* **2011,** *257*, 4291-4295.
15. Ramgir, N. S.; Late, D. J.; Bhise, A. B.; More, M. A.; Mulla, I. S.; Joag, D. S.; Vijayamohanan, K., *J Phys. Chem. B* **2006,** *110*, 18236-18242.
16. Schumann, J.; Eichelbaum, M.; Lunkenbein, T.; Thomas, N.; Alvarez Galvan, M. C.; Schlögl, R.; Behrens, M., *ACS Catal.* **2015,** *5*, 3260-3270.